journal

J. Am. Ceram. Soc., 77 [3] 711–16 (1994)

Binder Distribution in Macro-Defect-Free Cements: Relation between Percolative Properties and Moisture Absorption Kinetics

Jennifer A. Lewis* and Michelle Boyer*

Department of Materials Science and Engineering, University of Illinois at Urbana-Champaign, Urbana, Illinois 61801

Dale P. Bentz*

National Institute of Standards and Technology,* Gaithersburg, Maryland 20899

Macro-defect-free (MDF) cement is fabricated from a calcium aluminate cement and a poly(vinyl alcohol–acetate) (PVA) copolymer. For the composites studied, it was determined that the interphase regions comprised 63 vol% of the total binder content, while the bulk PVA regions comprised 37 vol% of this phase. Mercury intrusion porosimetry showed that a bimodal pore size distribution developed as binder was removed in increasing amounts from heat-treated samples. Larger pores with a characteristic diameter above 30 nm resulted from the removal of bulk PVA, whereas smaller pores approximately 5 nm in size resulted from the removal of water and PVA from the interphase regions. Simulation results obtained from a hard-core/soft-shell continuum percolation model of the MDF microstructure indicate that both the bulk PVA and interphase regions form percolative pathways through the system. Dramatic changes in both moisture absorption kinetics and flexural strength were observed only when a percolative network of larger pores was present in these composites. Hence, the bulk polymer regions are the dominant transport pathway for moisture in MDF cement. Based on this knowledge, processing guidelines have been developed to improve the moisture resistance of these materials.

I. Introduction

THE term "macro-defect-free" (MDF) refers to the absence of relatively large voids or defects that are normally present in conventional cement pastes because of entrapped air or inadequate mixing. A decade ago, Birchall and co-workers developed a novel processing method which avoids the formation of such strength-limiting defects.[1] Several cement/polymer systems have been processed by this technique, although the calcium aluminate cement/poly(vinyl alcohol–acetate) (PVA) copolymer system is most common.[2–6] MDF cements display unique properties relative to conventional cement pastes. For example, the flexural strength of MDF cement is about 200 MPa compared to approximately 10 MPa for hardened portland cement pastes.[2]

The polymeric phase in MDF cement serves many functions: (1) it acts as a rheological aid facilitating particle packing, (2) it fills the pore space between cement particles, and (3) it reacts chemically with cement hydration products to form an integral microstructural element referred to as the interphase regions.[4,7–10] It is believed that these regions, combined with the absence of large voids, are responsible for the high flexural strength of these materials. In the present work, we define the "binder phase" as both bulk polymer and interphase regions since each is responsible for binding unreacted cement grains.

Figure 1 shows micrographs of an MDF cement microstructure taken by transmission electron microscopy (TEM) and high-resolution electron microscopy (HREM).[8] The MDF microstructure consists of unreacted cement grains, comprised of both $CaAl_2O_4$ (CA) and $CaAl_4O_7$ (CA_2) where C = CaO, A = Al_2O_3, and H = H_2O, embedded in a plasticized poly(vinyl alcohol) matrix (refer to Fig. 1(a)). Interphase regions surround these cement grains, in which a fine dispersion of $Ca_2Al_2O_5{\cdot}8H_2O$ (C_2AH_8) crystallites (5–8 nm in size) resides in an amorphous matrix (refer to Fig. 1(b)). Based on these observations, the following hydration reaction has been proposed to occur during fabrication:[9]

$$2CaAl_2O_4 + 11H_2O \rightarrow Ca_2Al_2O_5{\cdot}8H_2O + 2Al(OH)_3 \quad (1)$$

Although MDF cements have been the subject of several investigations,[11–15] previous work neglected the complexity of its microstructure with respect to binder composition and distribution and their impact on performance properties.

In this paper, a series of computer simulations using a hard-core/soft-shell continuum percolation model are performed in combination with experiments to provide a greater understanding of the complex MDF microstructure and its effects on moisture absorption kinetics. Computer modeling provides a route for bridging the gap between the observable two-dimensional (2-D) microstructure described above and the three-dimensional (3-D) microstructure which determines such properties. This model was originally developed to allow the concept of excluded volume to be incorporated into continuum percolation studies[16] and it has been explored analytically and using computer simulations by several investigators.[17–19] The basic premise of the model is that particles are composed of impenetrable hard cores surrounded by soft shells which may overlap one another and may even partially envelop other hard cores without penetrating them. In the present work, the hard cores represent unreacted cement grains, the soft shells represent interphase regions, and the remaining space represents bulk PVA. These simulation results will provide a basis for interpreting our experimental observations.

The primary objectives of our study are twofold: (1) to develop a basic understanding of the percolative nature of both the polymer matrix and the interphase regions within the microstructure, and (2) to determine the relationship between the binder phase distribution and the moisture absorption kinetics of MDF cement.

M. Grutzeck—contributing editor

Manuscript No. 194601. Received May 5, 1993; approved October 18, 1993.
Presented at the 94th Annual Meeting of the American Ceramic Society, Minneapolis, MN, April 15, 1992 (Cements Division, Paper No. 37-T-92).
Supported by the National Science Foundation's Science and Technology Center for Advanced Cement-Based Materials (ACBM) through Grant No. DMR-91 2002.
*Member, American Ceramic Society.
*Building Materials Division, Building and Fire Research Laboratory, Technology Administration, U.S. Department of Commerce.

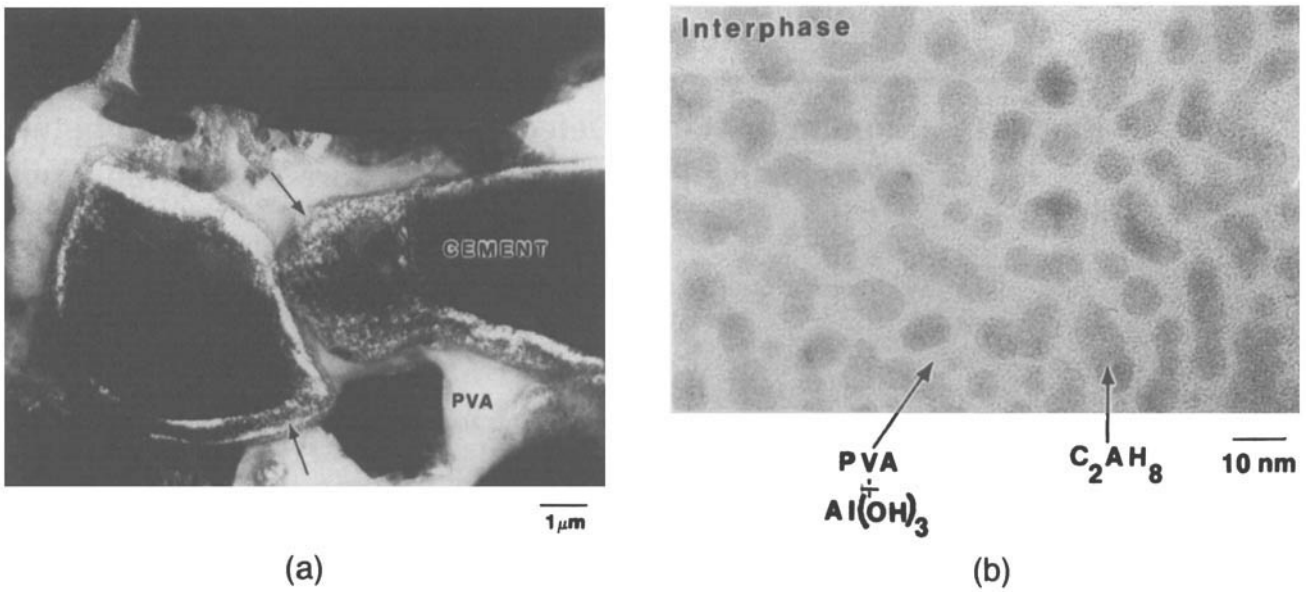

Fig. 1. Electron micrographs of the MDF cement microstructure (from Ref. 8): (a) bright-field TEM image of the microstructure [arrows indicate interphase regions] and (b) HREM micrograph of the interface between the cement grain and the PVA matrix.

II. Experimental Procedure

(1) Model Description

The hard-core/soft-shell continuum percolation model has been used successfully to model the percolation of interfacial zones in cement mortar and concrete.[20] For our application, the model system consists of a 3-D cube, 150 μm on a side, into which spherical particles are placed at random locations. Periodic boundaries are employed to eliminate edge effects so that any portion of a spherical particle which extends beyond the boundaries of the cube is reflected into the cube on the opposite face. Each particle consists of a variable-sized hard core surrounded by a constant-thickness soft shell. During random placement, the hard cores are not permitted to overlap, but overlap of the soft shells is permitted.

The size distribution of the hard cores was determined experimentally by measuring the particle size distribution of the calcium aluminate cement (Secar 71† powder from Lafarge Calcium Aluminates, Inc., Chesapeake, VA) used in our experiments. A dispersion was prepared which contained 3 vol% Secar 71 powder in A12 solvent (Micromeritics, Inc., Norcross, GA) and was analyzed by sedimentation (X-ray Sedigraph Model No. 5000E, Micromeritics, Inc., Norcross, GA). The cement particle size distribution ranged between 1 and 70 μm with a median size of 10 μm based on mass. This distribution was divided into seven size regions, in which hard-core particles were distributed uniformly by volume. Their volume was then reduced by 6.6% to account for the change in volume that results from hydration.

The percolation characteristics of the soft shells were evaluated in the following manner. Beginning at one edge of the top surface of the 3-D cube, the program finds all hard-core particles whose soft shells (interphase) overlap the top face of the cube. For each of these particles found, the program checks to see if any other hard-core particles present in the system contain soft shells which overlap this original soft-shell region. This process is repeated in an iterative fashion until all hard-core particles connected to the original particle via overlapping soft shells are located. Finally, this list of hard-core particles is examined to see if any of these particles contact the bottom face of the cube, indicating the existence of a percolated pathway through the system.

For the first set of simulations, it was determined that 3.005×10^5 hard-core spheres were required to produce a volume fraction of unreacted cement of 0.666, corresponding to the calculated value for the MDF cement samples (refer to the next section). The thickness of the soft-shell region surrounding each of the hard cores was varied between 100 and 500 nm in increments of 100 nm. For each soft-shell thickness, the hard-core/soft-shell computer program was executed to calculate the total volume of interphase material and its percolation characteristics. To verify the 3-D computer model, the volume fraction of the MDF composite occupied by the interphase regions was determined. Two areas of an HREM image of the interphase region[8] were digitized using a video camera and computer image processor. The resultant images were segmented into crystalline C_2AH_8 and amorphous $Al(OH)_3$ and PVA phases based on differences in gray level. From these images, their respective volume fractions could be determined. The volume fraction of C_2AH_8 combined with the total volume of this hydration product in the MDF system was then used to find the total volume occupied by interphase regions. By comparing these model results to experimental observations, the "best" interphase thickness could be determined as well as whether the interphase regions percolated for this thickness value.

Because the interphase regions consist of concentric spherical shells, their percolation characteristics can be easily determined in continuum space. This is not the case for the bulk PVA regions which consist of the space between particles and cannot be described in a simple geometric notation (e.g., a set of sphere centroids and radii). Thus, in the second set of simulation experiments, the continuum system corresponding to this best interphase thickness was digitized at resolutions of 150, 200, and 300 pixels per box side (i.e., 150 μm) resulting in total 3-D digital images comprised of 3.375×10^6, 8×10^6, and 27×10^6 pixels, respectively. The appropriate soft-shell thickness was determined from the first set of simulation experiments and was held constant in these experiments. Once digitized, a burning algorithm[21] was utilized to assess the connectivity of the remaining pore space (i.e., the bulk PVA matrix) at each resolution. To do this, all bulk PVA pixels are considered to be combustible. A "fire" is started at each combustible pixel on the top surface of the 3-D digital image and allowed to spread to all

†Certain commercial products are identified in this paper in order to adequately specify the experimental materials and procedures. In no case does such identification imply recommendation or endorsement by the National Institute of Standards and Technology, nor does it imply that the product is necessarily the best available for the purpose.

neighboring (± 1 in the x, y, and z directions) pixels which are combustible. If any bulk PVA pixel on the bottom surface of the digital image is burnt during the fire, a connected (or percolated) pathway of bulk PVA must exist through the 3-D microstructure. If a connected pathway exists, the fraction of the bulk PVA matrix that is percolated can be readily determined by counting the number of burnt pixels. These model results are then compared to the mercury intrusion porosimetry (MIP) results obtained on heat-treated MDF cement samples (refer to Experimental Procedure).

(2) Fabrication and Characterization of MDF Cement

The MDF cement samples investigated in this study were fabricated using the process developed by Birchall *et al.*[1] and optimized by Russell *et al.*[13] Their starting composition consisted of 150.0 g of calcium aluminate cement (Secar 71, Lafarge International, Chesapeake, VA), 10.5 g of PVA (Gohsenol KH-17s, Nippon Gohsei, Inc., Osaka, Japan), 1.05 g of glycerol (a PVA plasticizer), and 16.0 g of deionized water. The PVA had an average molecular weight of 105 000 g/mol and an acetate content of 22%. The individual constituents were first premixed in a planetary mixer. This was followed by high shear mixing on a twin roll mill to form sheets whose approximate dimensions were 300 mm × 150 mm × 1.5 mm. These sheets were then pressed at 5 MPa for 10 min and dried at 80°C in a forced air oven between plates for 24 h. Cylindrical samples (30 mm in diameter and 1.5 mm thick) were core drilled from the as-cured sheets. A more detailed description of this process is given by Russell *et al.*[13]

Several as-cured MDF cement samples approximately 30 mm in diameter and 1 mm in thickness were heated from room temperature to various maximum temperatures (T_{max} = 125–1000°C) at a rate of 1°C/min in air. Weight loss was measured following each furnace run to determine the amount of binder removed. Total volatile content was calculated from the weight loss observed for samples heated to 1000°C. MIP (Micromeritics Autopore II 9220, Norcross, GA) was performed on representative samples from each heat treatment to determine their pore structure. Additional heat-treated samples were exposed to relative humidities between 33% and 100% at 22°C and their weight gain was measured as a function of time. The average flexural strength of five samples from each heat treatment was obtained by (Instron Model No. 4502, Canton, MA) the biaxial flexural testing method.[22]

III. Results

(1) Binder Composition and Distribution

The binder phase holds the unreacted cement grains together within the MDF cement microstructure, and thus greatly influences the performance properties of this material. As the MDF samples are heated, volatile products are produced from the decomposition of plasticized-PVA and the hydration products, C_2AH_8 and $Al(OH)_3$. By comparing the weight loss (12.3%) measured upon heating samples to 1000°C to the weight of plasticized-PVA and water in the starting batch (15.75 wt%), one can see that some evaporation of water occurred during fabrication. The weight loss observed at 1000°C can be divided into contributions from plasticized-PVA decomposition (6.8 wt%) and loss of water (5.5 wt%) from hydration products in the interphase regions. From these data, the composition of the binder phase was determined in terms of the chemical components and their volatility as shown in Table I.

The distribution of the chemical components in the bulk PVA and interphase regions was determined in part from the digitized HREM images (refer to Fig. 1(b)). Image analysis showed that the volume fractions of crystalline (C_2AH_8) and amorphous phases ($Al(OH)_3$ and PVA) in the interphase regions were 0.625 and 0.375, respectively. It was assumed that $Al(OH)_3$ resided solely in the interphase regions, so that the amorphous phase could then be divided into the respective contributions from $Al(OH)_3$ and PVA as shown in Table II. The remaining plasticized-PVA in the MDF microstructure was assigned to the bulk PVA regions (refer to Table II).

(2) Percolative Nature of the 3-D Model Microstructure

The results of the simulation experiments are given in Table III, which shows the percolative nature of the interphase regions as a function of soft-shell thickness. The interphase regions percolate through the microstructure at all shell thicknesses evaluated as evidenced by a high degree of connectivity (>90%) even for the smallest shell thickness (100 nm) evaluated. To assess which of these soft-shell thicknesses best represented the interphase thickness present in MDF cement, we compared the volume of binder comprised of soft shells in Table III to the value determined experimentally for these samples (in Table II). For the shell thickness of 300 nm, the predicted value (61.9 vol%) was within a few percent of the experimental value (63.23 vol%). A cross-sectional view of the model system generated based on this shell thickness is shown in Fig. 2. The apparent variation in shell thickness shown in Fig. 2 is an artifact developed when a 2-D slice is taken through a 3-D system with constant shell thickness. However, since actual variations in interphase thickness have been observed in MDF,[8] this "best" shell thickness merely represents an average value for our samples.

While it is relatively easy to determine the percolation characteristics of the spherical hard-core/soft-shell particles in a continuum model, the percolation of bulk PVA is more difficult to assess, for reasons outlined previously. Thus, the continuum system with a shell thickness of 300 nm was digitized at several resolutions to determine the percolative nature of bulk PVA using a conventional digital-image-based burning algorithm.[21] As the grid size (number of pixels per box side) increases, the volume fraction of PVA remains constant while the percolated fraction is observed to increase significantly as shown in

Table I. Final Composition of MDF Cement

Component	Composition wt%	Composition vol%
Unreacted cement (CA, CA_2)	78.7	66.6
Binder phase		
C_2AH_8	10.1	13.2
$Al(OH)_3$	4.4	4.6
Plasticized-PVA	6.8	15.6
Nonvolatiles	87.7	70.4
Volatiles (in binder phase)		
Plasticized-PVA	6.8	15.6
H_2O	5.5	14.0

Table II. Distribution of Constituents in the Binder Phase in MDF Cement

Constituent	Total binder phase (vol%)	Interphase region (vol%)
Interphase regions	63.23	
C_2AH_8	39.52	62.5
$Al(OH)_3$	13.77	21.8
PVA	9.94	15.7
PVA (bulk) matrix	36.77	

Table III. Simulation Results on Interphase Region Properties in MDF Cement

Interphase region thickness (nm)	Volume fraction of interphase region	Connected fraction of interphase region	Binder in interphase region (%)
100	0.0675	0.899	20.2
200	0.1390	0.990	41.6
300	0.2067	0.9995	61.9
400	0.2615	0.999996	78.2
500	0.2987	1.0	89.4

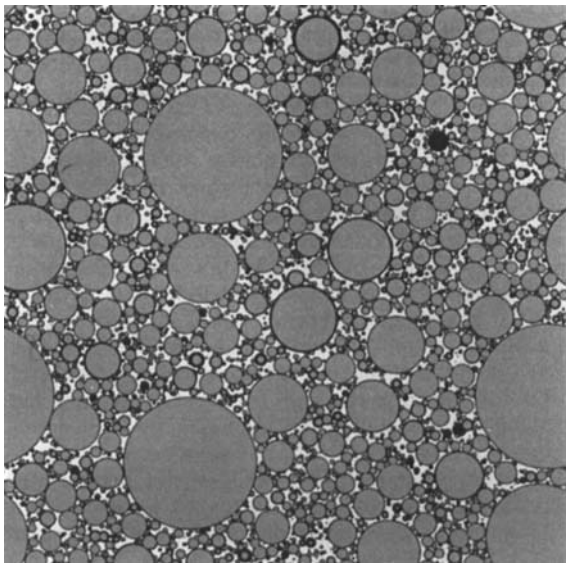

Fig. 2. Two-dimensional view of the simulated MDF cement microstructure, where the unreacted cement grains (hard cores) are shown in gray, the interphase regions (soft shells) are shown in black, and the bulk PVA matrix is shown in white.

Table IV. The resolution required to observe a high level of percolation of this region is directly related to the length scale of PVA-filled pores. These simulations yielded a value of 500 nm for this length, which is in excellent agreement with the experimental results described in the next section.

(3) Influence of MDF Microstructure on Moisture Absorption

The amount of binder removed (based on the total possible weight loss) as a function of temperature is shown in Table V for each set of heat-treated MDF cement samples. The maximum heat-treatment temperature (T_{max}) determined not only how much binder was removed, but from which region in the microstructure removal occurred. Water is the only volatile constituent removed from samples heated to 125°C since this temperature is below the decomposition temperature of PVA and the diffusivity of larger volatile constituents in the system

Table IV. 3-D Burning Algorithm Results for Connectivity of PVA Matrix Regions in MDF Cement

Grid size	Resolution (nm)	Volume fraction of PVA matrix in MDF cement	Fraction of PVA matrix connected to top	Fraction of PVA matrix percolated
150	1000	0.1274	0.0299	0
200	750	0.1273	0.7130	0.6954
300	500	0.1274	0.9568	0.9561

Table V. Amount of Binder Removed from the Heat-Treated MDF Cement Samples

T_{max} (°C)	Binder removed relative to total binder weight (wt%)
	0.0
125	12.8
175	28.6
200	35.1
250	38.8
300	55.0
350	63.9
400	75.0
1000	100.0

(e.g., glycerol) should be several orders of magnitude lower than that of water.[23] At higher temperatures ($T_{max} \geq 175$°C), water, glycerol, and PVA decomposition products were removed simultaneously from these samples. Hence over the temperature range examined, we produced samples where material was removed either selectively from the interphase regions or from both the interphase and the bulk PVA regions.

Figure 3 depicts the weight gain as a function of time for heat-treated MDF cement samples exposed to 93% relative humidity at 22°C. Here we report only the data measured at 93% rh, though the same basic trends in weight gain as a function of time were observed for all relative humidities (33–100% rh) evaluated. There are several differences in the moisture absorption behavior of these samples. First, their weight gain during the first few days of moisture exposure differed dramatically. A rapid weight gain (≈2–4 wt%) was observed for samples heated above 125°C. In contrast, a much lower weight gain (<0.5 wt%) was observed for non-heat-treated samples (standard MDF) and for those heated to only 125°C. Secondly, there was little difference in weight gain between these two samples. In fact, samples heated to 125°C exhibited a slightly higher resistance to moisture absorption over the duration of this experiment as compared to standard MDF cement. Finally, the weight gain of all samples leveled off at longer periods of exposure.

The existence of mechanistic differences between the moisture absorption kinetics of the heat-treated MDF samples is observed in Fig. 4, which shows their weight gain as a function of the square root of time. Each curve in Fig. 4 was fitted by least-squares analysis to assess whether the moisture absorption process was diffusion-controlled. It is evident by the correlation coefficient (R) determined for each curve, that only standard MDF and those samples heated to 125°C displayed diffusion-controlled kinetics during this time period.

The incremental intrusion volume as a function of pore diameter is shown in Fig. 5, which illustrates the development of a bimodal pore size distribution as increasing amounts of binder were removed. For comparison, the incremental intrusion curve for standard MDF is also included, which shows that these samples contained minimal open porosity. The bimodal pore distribution was divided into two regions: one associated with pores in the interphase regions and the other associated with pores in the bulk PVA regions. A characteristic pore size (D_{pore}), defined by the maximum of the incremental intrusion curve, was determined for each region and these sizes correlated well to features present in the MDF microstructure. For example, the smaller pores ($D_{pore} \approx 3$–7 nm) are approximately the same size of the C_2AH_8 crystallites or the spacing between crystallites in the interphase regions (refer to Fig. 1(b)), whereas the larger pores

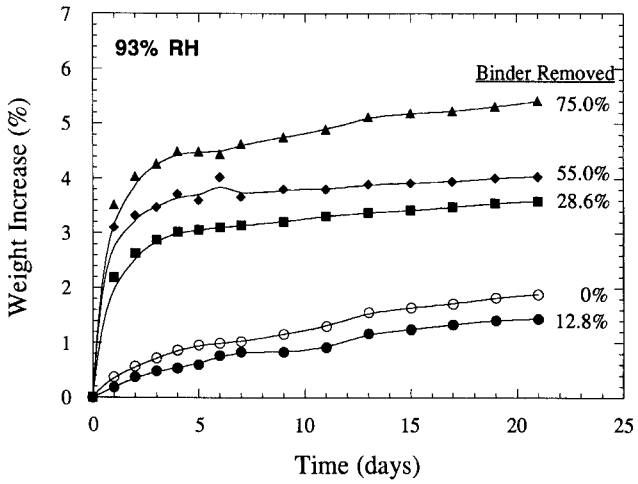

Fig. 3. Plot of weight gain as a function of time for heat-treated MDF cement samples exposed to 93% relative humidity.

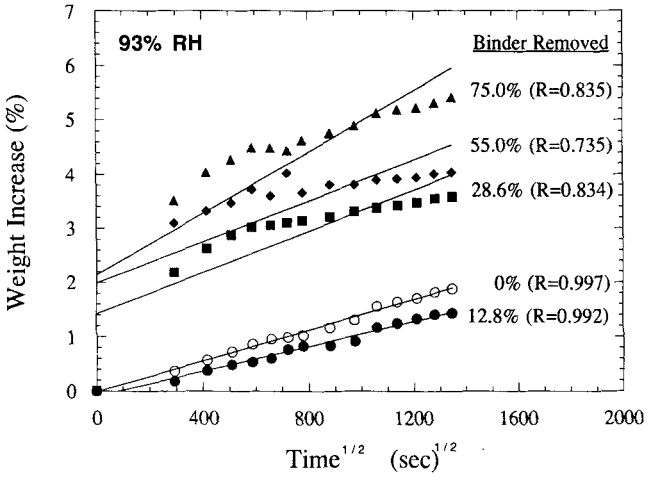

Fig. 4. Plot of weight gain as a function of (time)$^{1/2}$ for heat-treated MDF cement samples exposed to 93% relative humidity.

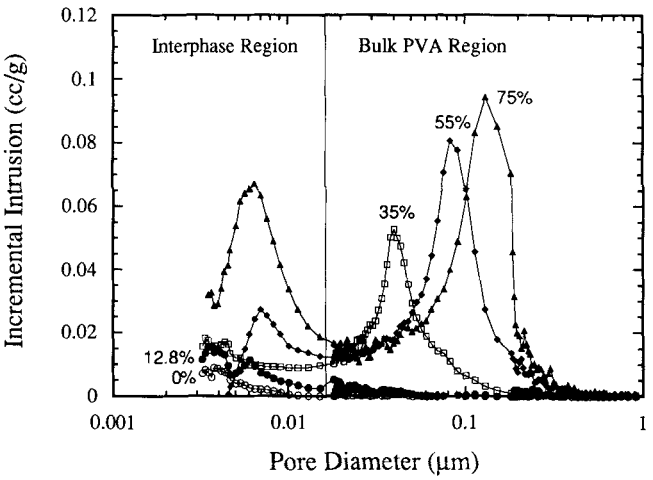

Fig. 5. Mercury intrusion porosimetry results which show the incremental intrusion as a function of pore diameter for the heat-treated MDF cement samples.

($D_{pore} \geq 30$ nm) are of the same size as bulk PVA-filled interstices formed between unreacted cement particles. Hence, samples heated to 125°C exhibited porosity only in the interphase region, whereas samples heated above 125°C exhibited porosity in both regions. Finally, the maximum pore diameter (D_{max}) was also determined for these samples and is plotted as a function of binder removed in Fig. 6. D_{max} is the pore diameter where the intrusion of mercury is first observed based on cumulative intrusion curves. D_{max} ranged between 13.7 and 533 nm for samples with 0% to 100% binder removed, respectively.

The average flexural strengths of heat-treated MDF samples as a function of binder removed are shown in Fig. 7. The standard MDF cement samples had an average strength of 220 MPa. Upon partial degradation of the interphase region (125°C heat treatment), the flexural strength was reduced by approximately 33%. This result appears to contradict earlier work by Poon *et al.*[11] They attributed the weight loss observed in MDF samples heated to similar temperatures (<200°C) to loss of water and associated the dramatic reduction (≈75%) in flexural strength that they observed to water removal. However, since the resulting pore structure of their samples was not characterized, it is unclear whether only water loss occurred in their experiment. In the present study, we observed a significant reduction in flexural strength to approximately 15% of its initial value only upon removal of bulk PVA.

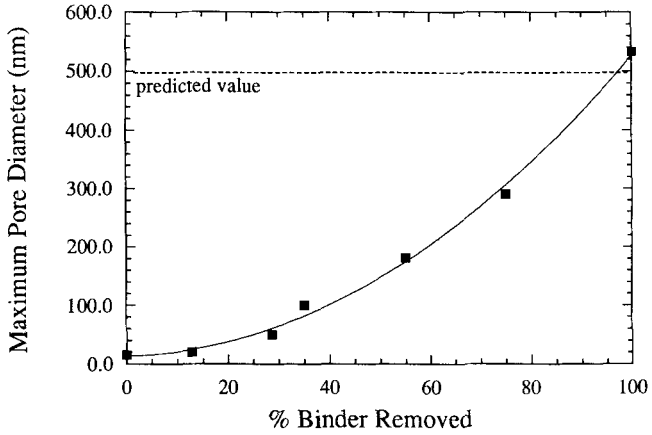

Fig. 6. Maximum pore diameter as a function of binder removed from the heat-treated MDF cement samples.

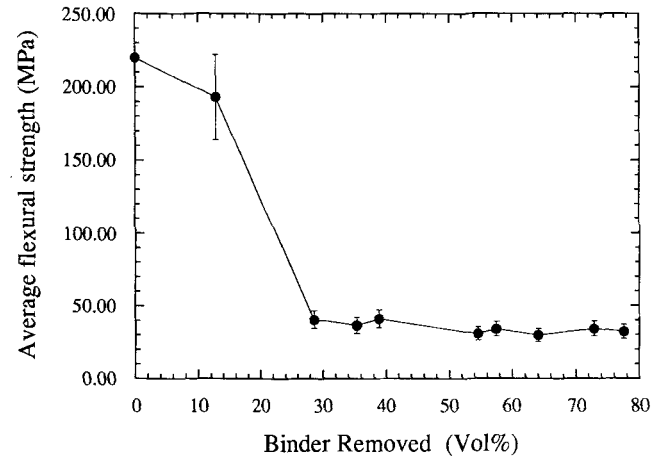

Fig. 7. Plot of average flexural strength as a function of binder removed for the heat-treated MDF cement samples.

IV. Discussion

A fundamental understanding of how moisture is transported from the sample surface to its interior through the binder phase has emerged from our work. Through computer modeling, we have shown that both polymer and interphase regions form percolative pathways through the MDF microstructure. This was supported by MIP measurements which illustrated that connected porosity developed in both regions upon their removal from MDF cement. Because of the hygroscopic nature of plasticized-PVA, this phase is thought to be mainly responsible for moisture transport in MDF cements.[13,15] We have shown that the polymeric phase is distributed such that approximately 20% of it resides in the interphase regions, while the remainder resides in bulk polymer regions (refer to Table II). The experiments described above allow the contributions of each of these regions to moisture transport to be separated. As we will discuss below, our results indicate that only bulk polymer regions facilitate moisture transport in this system.

Because MIP detects only *open porosity* (i.e., pores connected to the sample surface), all heat-treated MDF samples contained pores which could serve as "fast" diffusion pathways to the sample interior (refer to Fig. 5). Two types of porosity were observed: fine-scale porosity developed in the interphase regions and large-scale porosity developed in the bulk polymer regions. Since the diffusivity of water vapor in these pores is several orders of magnitude higher than the diffusivity of water through the plasticized-PVA or the interphase regions, we expected all heat-treated samples to exhibit enhanced moisture

through the plasticized-PVA or the interphase regions, we expected all heat-treated samples to exhibit enhanced moisture absorption kinetics relative to standard MDF cement. In addition, we expected this enhancement would increase with increasing pore content. However, our experimental observations (see Fig. 3) indicate that these trends were observed only for samples containing large-scale porosity ($D_{pore} \geq 30$ nm). In fact, samples that contained only fine-scale porosity ($D_{pore} \approx 5$ nm) actually exhibited improved moisture resistivity relative to standard MDF cement as well as similar diffusion-controlled kinetics. This was observed even though capillary condensation of moisture may occur in such pores. The Kelvin equation predicts that moisture could condense in pores less than 15 nm in diameter for these experimental conditions (i.e., 93% rh at 22°C); however, at lower relative humidities this process will not occur. Therefore, since the same basic trends in weight gain as a function of time were observed for all relative humidities evaluated (33–100% rh), capillary condensation does not significantly impact the interpretation of our results. The observed enhanced moisture resistivity of samples containing only fine-scale porosity not only supports this statement, but suggests that the transport of moisture in the PVA located in the interphase region is significantly different from that found in the bulk. In fact, experimental evidence of chemical differences between the PVA in these two regions has been previously observed[9] which could account for our observations. In this system, the bulk PVA regions clearly dominate moisture absorption kinetics, since it is only upon the development of pores in these

Finally, we have found excellent agreement between the computer simulation and experimental results of this study. For example, both simulations and experiments indicated that the binder phase elements form connected pathways through the MDF microstructure. In addition, the computer simulations predicted that a resolution of 500 nm would be required to resolve the connectivity of the bulk PVA matrix. In comparison, MIP showed that the maximum diameter of the PVA-filled pores was approximately 533 nm for samples heated to 1000°C (refer to Fig. 6). The overall correlation between simulation and experimental results, in combination with knowledge of the 3-D MDF microstructure afforded by the hard-core/soft-shell continuum percolation model, supports its continued use in future investigations.

V. Conclusions

To develop processing strategies that lead to improved moisture resistance of MDF cements, one must first understand how moisture is transported from the sample surface to its interior. In this study, we have elucidated a clear picture of the 3-D MDF microstructure, its binder composition and distribution, as well as its impact on moisture absorption kinetics. We determined that although the interphase regions form a percolative pathway through the MDF cement microstructure, their contribution to the transport of moisture is limited. In contrast, the bulk polymer regions have a significant effect on moisture absorption, providing the dominant transport pathway.

The knowledge gained from our work suggests that modifying the binder phase of MDF cement such that the interphase to bulk PVA ratio increases should yield materials with improved moisture resistivity. In such samples, a nonpercolative distribution of bulk PVA would result, thereby inhibiting moisture transport to their interior. An alternative approach is to chemically modify bulk organic regions rather than disrupt their connectivity in the microstructure. For instance, the PVA chemistry could be changed through the addition of a cross-linking agent also leading to improved moisture resistivity. Presently, we are evaluating the merit of each of these strategies by assessing their effects on the processing, microstructural development, and performance of MDF cements.

Acknowledgments: We would like to thank Dr. O. O. Popoola for granting us permission to use his high-resolution electron microscopy results. We would also like to thank Professors J. F. Young and M. Berg for several fruitful discussions during the course of this work, and Scott Covey for his assistance in particle size analysis.

References

[1]J. D. Birchall, A. J. Howard, and K. Kendall, "Cement Composition and Product," U.S. Pat. No. 4410366, 1983.

[2]K. Kendall, A. J. Howard, and J. D. Birchall, "The Relationship between Porosity, Microstructure and Strength, and the Approach to Advanced Cement-Based Materials," *Philos. Trans. R. Soc. London*, **A310,** 139–53 (1983).

[3]R. N. Edmonds and A. J. Majumdar, "The Hydration of and Aluminous Cement with Added Polyvinyl Alcohol–Acetate," *J. Mater. Sci.*, **24,** 3813–18 (1989).

[4]J. D. Birchall, A. J. Howard, and K. Kendall, "Strong Hydraulic Cements," *Br. Ceram. Soc. Proc.*, **32,** 25–32 (1982).

[5]N. McN. Alford and J. D. Birchall, "Properties and Potential Applications of Macro-Defect-Free Cement," *Mater. Res. Soc. Symp. Proc.*, **42,** 265–76 (1985).

[6]D. M. Roy, "New Strong Cement Materials: Chemically Bonded Ceramics," *Science*, **35,** 651–57 (1987).

[7]J. D. Birchall, "Cement in the Context of New Materials for an Energy-Expensive Future," *F.R.S. Philos. Trans. R. Soc. London*, **A310,** 31–42 (1983).

[8]O. O. Popoola, W. M. Kriven, and J. F. Young, "High Resolution Electron Microscopy and Microchemical Characterization of Polyvinyl Alcohol Acetate/Calcium Aluminate Composite (Macro-Defect-Free Cement)," *Ultramicroscopy*, **37,** 318–25 (1991).

[9]O. O. Popoola and W. M. Kriven, "Interfacial Structure and Chemistry in a Ceramic/Polymer Composite Material," *J. Mater. Res.*, **7** [6] 1545–52 (1992).

[10]S. A. Rodger, S. A. Brooks, W. Sinclair, G. W. Grooves, and D. D. Double, "High Strength Cement Pastes: Part 2, Reactions During Setting," *J. Mater. Sci.*, **20,** 2853–60 (1985).

[11]C. S. Poon, L. E. Wassell, and G. W. Groves, "Stability of Macro-Defect-Free Cement," *Mater. Sci. Technol.*, 993–96 (1988).

[12]C. M. Cannon and G. W. Groves, "Time-Dependent Mechanical Properties of High-Strength Cements," *J. Mater. Sci.*, **21,** 4009–14 (1986).

[13]P. P. Russell, J. Shunkwiler, M. Berg, and J. F. Young, "Moisture Resistance of Macro-Defect-Free Cement," *Ceram. Trans.*, **16,** 501 (1991).

[14]G. V. Chandrashekhar, E. Cooper, and M. W. Shafer, "Dielectric Properties of Macro-Defect-Free (MDF) Cements," *J. Mater. Sci.*, **24,** 3356–60 (1989).

[15]S. Goto, H. Koyata, M. Daimon, E. Yasuda, and S. Kimura, "Diffusion of Moisture in MDF Cement," *MRS Int. Meet. Adv. Mater.*, **13,** 207–12 (1989).

[16]I. Balberg, "Recent Developments in Continuum Percolation," *Philos. Mag. B*, **56** [6] 991–1003 (1987).

[17]I. Balberg and N. Binenbaum, "Invariant Properties of the Percolation Thresholds in the Soft Core-Hard Core Transition," *Phys. Rev. A*, **35** [12] 5174–77 (1987).

[18]S. B. Lee and S. Torquato, "Porosity for the Penetrable-Concentric-Shell Model of Two-Phase Disordered Media: Computer Simulation Results," *J. Chem. Phys.*, **89** [5] 3258–63 (1988).

[19]P. A. Rikvold and G. Stell, "Porosity and Specific Surface for Interpenetrable-Sphere Models of Two-Phase Random Media," *J. Chem. Phys.*, **82** [2] 1014–20 (1985).

[20]K. A. Snyder, D. N. Winslow, D. P. Bentz, and E. J. Garboczi; pp. 265–70 in *Advanced Cementitious Systems: Mechanisms and Properties*. Edited by F. P. Glasser *et al.* Materials Research Society, Pittsburgh, PA, 1992.

[21]D. Stauffer, *Introduction to Percolation Theory*. Taylor and Francis, London, U.K., 1985.

[22]J. B. Wachtman, W. Capps, and J. Mandrel, "Biaxial Flexure Tests of Ceramic Substrates," *J. Mater.*, **7,** 188–94 (1972).

[23]J. A. Lewis and M. J. Cima, "Diffusivity of Dialkyl Phthalates in Plasticized PVB: Impact on Binder Thermolysis," *J. Am. Ceram. Soc.*, **73** [9] 2702–707 (1990). □